APPLIED AND ENVIRONMENTAL MICROBIOLOGY, June 1994, p. 1859–1866
0099-2240/94/$04.00+0

Vol. 60, No. 6

Nitrogen Fixation and Hydrogen Metabolism in Relation to the Dissolved Oxygen Tension in Chemostat Cultures of the Wild Type and a Hydrogenase-Negative Mutant of *Azorhizobium caulinodans*

FRED C. BOOGERD,* MARIJKE M. A. FERDINANDY-VAN VLERKEN, CRISPEN MAWADZA,†
ANNEMIEKE F. PRONK, ADRIAAN H. STOUTHAMER, AND HENK W. VAN VERSEVELD

Department of Microbiology, Institute for Molecular Biological Sciences, BioCentrum Amsterdam, Vrije Universiteit, 1081 HV Amsterdam, The Netherlands

Received 17 November 1993/Accepted 30 March 1994

Both the wild type and an isogenic hydrogenase-negative mutant of *Azorhizobium caulinodans* growing ex planta on N_2 as the N source were studied in succinate-limited steady-state chemostat cultures under 0.2 to 3.0% dissolved O_2 tension. Production or consumption of O_2, H_2, and CO_2 was measured with an on-line-connected mass spectrometer. In the range of 0.2 to 3.0%, growth of both the wild type and the mutant was equally dependent on the dissolved O_2 tension: the growth yield decreased, and the specific O_2 consumption and CO_2 production increased. A similar dependency on the dissolved O_2 tension was found for the mutant with 2.5% H_2 in the influent gas. The H_2/N_2 ratio (moles of H_2 evolved per mole of N_2 consumed via nitrogenase) of the mutant, growing with or without 2.5% H_2, increased with increasing dissolved O_2 tensions. This increase in the H_2/N_2 ratio was small but significant. The dependencies of the ATP/N_2 ratio (moles of ATP consumed per mole of N_2 fixed) and the ATP/$2e^-$ ratio [moles of ATP consumed per mole of electron pairs transferred from NAD(P)H to nitrogenase] on the dissolved O_2 tension were estimated. These dependencies were interpreted in terms of the physiological concepts of respiratory protection and autoprotection.

Aerobic diazotrophs have established ways to unite the process of N_2 fixation with the occurrence of H_2 and O_2 inside their cells, because the latter two gaseous molecules can be potentially detrimental for diazotrophy. The reduction of N_2, catalyzed by nitrogenase, yields H_2 as a by-product (see reference 41). High N_2 pressures, even as high as 50 atm (1 atm = 101.29 kPa), do not prevent H_2 evolution during N_2 fixation (31). A stoichiometry of 1 mol of H_2 evolved per mol of N_2 consumed is considered obligatory because of the displacement of H_2 by N_2 when N_2 binds at nitrogenase (22, 23, 37, 38). This H_2/N_2 ratio (moles of H_2 evolved per moles of N_2 consumed through nitrogenase catalysis) only represents a minimum value. Under various experimental conditions, in vitro as well as in vivo, H_2/N_2 ratios higher than 1 have been observed (see references 14, 26, 32, and 41). Reduction of N_2 and H^+ by nitrogenase requires a strong reductant and a high energy input (14). Aerobic N_2-fixing microorganisms produce an electron donor (ferredoxin or flavodoxin) with a low redox potential (E_h is about -500 mV) to reduce the nitrogenase reductase. Although the mechanism of reduction of this electron donor is itself still unknown (14), NAD(P)H, the proton-motive force, and/or ATP might have some involvement (34). The reduced nitrogenase reductase transfers its electron to nitrogenase with concomitant hydrolysis of 2 ATP. The in vivo overall ATP/$2e^-$ ratio is defined as the number of ATP molecules needed to transfer two electrons from the reductant [NAD(P)H] to the substrate (N_2 or H^+) (5). Bioenergetically, production of H_2 via nitrogenase means a loss of energy and electron equivalents. The H_2/N_2 ratio is an important parameter involved in the energetics of nitrogen fixation (2, 32). Oxygen can be either beneficial or detrimental for N_2-fixing microorganisms. In obligate aerobic microorganisms, O_2 serves as a terminal electron acceptor in the oxidation of electron equivalents, which process is coupled to the formation of the proton-motive force. At the same time, O_2 may inhibit the activity and repress the synthesis of nitrogenase (18).

Azorhizobium caulinodans is capable of growing ex planta on N_2 as the sole N source in continuous cultures at dissolved O_2 tensions (DOTs) of up to 4% and at specific growth rates of up to 0.15 h^{-1} (1, 3, 11, 13, 33). In this respect, it is a unique species among the rhizobia, because *Bradyrhizobium* and *Rhizobium* spp. ex planta do not grow on N_2. *A. caulinodans* contains an H_2-induced uptake hydrogenase which is active during growth on N_2 as the N source (7, 33). In consequence, H_2 produced as the by-product of N_2 reduction by nitrogenase is usually not detected in the effluent gas of nitrogen-fixing cultures. The uptake hydrogenase oxidizes H_2 and uses ubiquinone as the electron acceptor (7, 33). We have previously described the isolation of Tn*5*-induced hydrogenase-negative (Hup^-) mutants (W series) of *A. caulinodans* (5). With these mutants, H_2/N_2 ratios ranging from 1.2 to 1.9 have been measured in chemostat cultures in which growth at a low and constant DOT occurred under various limitations (5). The present series of experiments was designed to examine H_2 metabolism and N_2 fixation in relation to the DOT in chemostat cultures of the wild type and another hydrogenase-negative mutant of *A. caulinodans*.

* Corresponding author. Mailing address: Free University, Faculty of Biology, De Boelelaan 1087, 1081 HV Amsterdam, The Netherlands. Phone: 31-20-4447193. Fax: 31-20-4447193. Electronic mail address: fcb@bio.vu.nl.

† Present address: Department of Biochemistry, University of Zimbabwe, Mount Pleasant, Zimbabwe.

MATERIALS AND METHODS

Bacterial strains. The wild-type strain used was *A. caulinodans* ORS571 (10). The hydrogenase-negative mutant used in this study (U58) was constructed from a previously described mutant (5). The latter Hup$^-$ mutant (W58) was first thought to have been constructed from ORS571 (5) but was in fact derived from a spontaneous (ORS571-CY1) mutant (11, 17). Strain ORS571-CY1 was still able to grow on N_2 ex planta but produced high concentrations (25 to 30%, wt/wt) of poly-β-hydroxybutyrate (PHB) in free-living cultures (11). Mutant U58 (Hup$^-$ Nif$^+$ Nod$^+$ Fix$^+$ Km^r) was constructed by U. Hilgert (Max Planck Institut für Züchtungsforschung, Cologne, Germany) by homologous recombination in bona fide ORS571 (17). It accumulated PHB in normal concentrations (around 10%, wt/wt) in succinate-limited, free-living cultures (this study).

Media. For succinate-limited chemostat cultures, media contained 25 or 50 mM succinic acid, 9.6 mM K_2HPO_4, 6.4 mM KH_2PO_4, 1.0 mM $MgSO_4$, 195 μM nicotinic acid, 25 μM citric acid, 21 μM $NaMoO_4$, 20 μM $FeSO_4$, 8.4 μM Ca pantothenate, 0.2 μM biotin, and 2 ml of a stock solution of trace elements per liter. The stock solution contained (per liter) 25 g of NaCl, 20 g of $CaCl_2 \cdot 2H_2O$, 1.25 g of $MnSO_4 \cdot H_2O$, 0.35 g of $ZnSO_4 \cdot 7H_2O$, 0.1 g of $NiCl_2 \cdot 6H_2O$, 0.07 g of $CoCl_2 \cdot 6H_2O$, 0.06 g of $CuSO_4 \cdot 5H_2O$, and 0.015 g of H_3BO_3. Large (20-liter) glass vessels containing all of the substances mentioned, except the phosphate salts, were filled with 17.5 liters of deionized water, and the contents were boiled for 6 h. The phosphate salts were dissolved in 0.5 liter of deionized water, autoclaved for 15 min at 120°C, and then added to the medium vessel. For U58 cultures, filter-sterilized kanamycin (1 mg/liter) was added to all of the media.

Chemostat. A 2-liter glass fermentor (Applikon BV) with a working volume of 1 liter was used. The growth temperature was maintained at 35°C by circulation of water through the internal frame of the head plate (stainless steel), which contained threaded apertures for mounting of controlling devices. The pH of the culture was continuously measured with a pH electrode (Ingold) and regulated at 6.8 or 7.0 by addition of 2 M KOH or HCl. The DOT was measured with a polarographic O_2 sensor (Ingold) and controlled at a preset value (0.20 to 3.00%) by using an O_2 controller (512; Powers Process Controls) by regulating the rotational speed of the stirrer with a certain proportional and integrating characteristic. Gas was sparged through the culture via a submerged pipe. Two six-blade turbine stirrers and three baffles dispersed the influent gas. The stirrer speed was 600 to 900 rpm. The influent gas was composed of N_2 (85 to 95%), O_2 (5 to 15%), and, if necessary, H_2 (2.5%). The desired composition of the gas was realized by mixing gases from various supplies. These flows were controlled with mass flow controllers (5850TR; Brooks Instruments). Mixing occurred after these controllers in a special filter (4TF-F2-7; NUPRO Co.), where two or three gas flows were united. After mixing, the gas stream was split into major and minor streams. The major flow (5 or 20 liters/h at 0°C) was directed towards another mass flow controller, which was installed just before the sparger and controlled the flow through the fermentor vessel. The effluent gas flow was led via an overflow vessel (1 liter) to the mass spectrometer. The minor reference flow was transferred straight to the mass spectrometer at a flow rate of at least 5 liters/h (0°C). Medium was added to the fermentor vessel at a flow rate of 100 ml/h by using a peristaltic pump (101U-R; Watson-Marlow). Culture overflow was removed via a drain plug that was directed at the liquid surface of the culture by using another peristaltic pump.

TABLE 1. Types of steady-state chemostat cultures of ORS571 and U58

Type of chemostat culture	No. of cultures	*A. caulinodans* strain	% H_2 in influent gas	Influent gas flow rate (liters/h)
1	13	U58	0	5
2	10	U58	0	20
3	8	U58	2.5	5
4	17	ORS571	0	20

Different types of chemostat cultures of ORS571 and U58. All steady-state chemostat cultures had the following conditions in common: pH 6.8 to 7.0; temperature, 35°C; $D = \mu = 0.1\ h^{-1}$; limiting factor, succinate; N source, N_2. No differences in growth parameters were observed for bacterial cells grown on media containing 25 or 50 mM succinate. The variables (apart from the DOT) among the four types of cultures comprised the *A. caulinodans* strain used, the number of chemostat cultures, the percentage of H_2 in the influent gas, and the influent gas flow rate (Table 1). These variables were chosen for the following reasons. Chemostat cultures were established with and without H_2 in the influent gas to estimate the effect of H_2 on the growth of U58 as a function of the DOT. The influent gas flow rate was lowered from 20 to 5 liters/h (0°C), reflecting the practical advantages of more precise measurement and more sensitive mass spectrometric detection of H_2 production.

Mass spectrometer. The effluent and influent gases were frequently (at least every 10 min) analyzed for N_2, O_2, Ar, CO_2, and H_2 with an on-line-connected, single-detector, magnetic-sector mass spectrometer (MM8-80F; VG Instruments). The composition of the effluent gas was corrected for changes in the volume of the gas (39). The difference between percentages of particular gases in the influent and corrected effluent gas streams, together with the flow rate of the influent gas (0°C), was used to balance the gas phase for each chemostat culture. From these balances, the production or consumption of CO_2, H_2, and O_2 was calculated. In the case of CO_2, a correction was made for removal of CO_2 and HCO_3^- from the vessel via the liquid culture effluent (25). This correction was particularly substantial when the low gas flow rate (5 liters/h) was used. The mass spectrometer was calibrated by using He as the background and a calibration mixture containing 1.00% CO_2, 1.00% Ar, 0.200% H_2, and 20.00% O_2, balanced with N_2 (BOC). After calibration, this mixture was regularly measured to check for changes. Moreover, another calibration mixture containing 3.50% O_2 and 5.00% H_2 (Union Carbide) was used to control the linearity of the O_2 and H_2 signals in the mass spectrometer.

Measurement of the H_2/N_2 ratio in the chemostat-mass spectrometer. The H_2/N_2 ratio (moles of H_2 evolved per mole of N_2 consumed) was estimated with the help of the equation $H_2/N_2 = (2.8 \times qH_2)/(\mu \times \%N)$, in which qH_2 is the specific rate of H_2 production (millimoles of H_2 gram of dry weight $[DW]^{-1}$ $hour^{-1}$), %N is the mean N percentage of the dry weight of cells, μ is the specific growth rate, and 2.8 converts grams of N into millimoles of N_2. To minimize leakage of H_2, stainless steel pipes were used to connect the gas-mixing station, via the chemostat vessel, with the mass spectrometer (culture channel, about 10 m) and to connect the gas-mixing station directly with the mass spectrometer (reference channel, about 6 m). In this chemostat-mass spectrometer system, 99% of the hydrogen gas was retained.

Analyses. Bacterial DW was measured by filtration on

constant-weight membrane filters (8). Three samples (15 or 25 ml) of every chemostat culture were used to determine the mean DW. The PHB content of cells was measured either colorimetrically (21) or gas chromatographically (30). Two 15-ml samples of every chemostat culture were taken, and cells were centrifuged at 10,000 × *g* and 4°C. The resulting bacterial pellets were analyzed for PHB. The elementary composition of dried cells (C, H, and N) was determined with an Element Analyzer (Carlo Erba Instrumentazione, Milan, Italy). Cells were washed twice with cold water and dried in tin capsules. Two samples, each of approximately 1.5 mg of dried cells, were analyzed for each chemostat culture. The ash content of dried cells was taken as 5%. The percentage of O of dried cells was calculated by subtracting the sum of the percentages of C, H, N, and ash from 100%. The percentages of C, H, N, and O of dried cells were used to calculate the elementary composition of the biomass. The biomass was defined as the substance of dried cells minus PHB, an internal product, which was taken into account in the assimilation equation (11). Residual succinate present in the culture fluid was determined indirectly from the organic carbon content with a Total Organic Carbon Analyzer (915A; Beckman Instruments Inc.). ORS571 does not make any detectable substances other than CO_2, biomass, and PHB from succinate (6).

Precultures. The medium used for starter cultures had the same composition as that used for continuous cultures, except for the presence of 3 mM NH_4Cl. After inoculation of this medium (150 ml in 500-ml serum bottles) with ORS571 or U58, the bottles were closed and placed in a rotary shaking incubator (35°C). After 2 or 3 days of growth (optical density at 660 nm, 1), ammonium was completely consumed, atmospheric O_2 was lowered, and derepression of nitrogenase was achieved.

RESULTS

Elementary cell composition. The percentages of C, H, N, and O of dried bacterial cells of *A. caulinodans* were determined in 25 samples of ORS571 and 28 samples of U58. These samples were all taken from N_2-fixing, succinate-limited, steady-state chemostat cultures, with or without H_2 in the influent gas, and maintained under a 0.2 to 3.0% DOT. Among these cultures, the percentages of C, H, N, and O showed little change with the growth conditions imposed. Therefore, all 53 CHNO analyses were combined and used to calculate the mean percentages of C, H, N, and O and the standard errors of the means. The percentages were as follows: C, 46.5% ± 0.1%; H, 6.72% ± 0.02%; N, 9.38% ± 0.05%; O, 32.4% ± 0.2%. Likewise, the percentage (wt/wt) of PHB varied only slightly with the growth conditions imposed. All 61 PHB analyses were combined and used to calculate the mean percentage of PHB and its standard error: 10.5% ± 0.5%. Subsequently, the mean elementary cell composition was calculated. In this calculation, the reserve-material PHB was considered an internal bacterial product and was therefore not included in the elementary cell composition. The elementary cell composition of PHB-less cells of *A. caulinodans* was estimated to be, on a C_1 basis, $CH_{1.77}N_{0.197}O_{0.53}$. This cell formula was used in the calculation of the carbon and redox balances in accordance with the macroscopic balance method (40). These balances indicated reasonable-to-good consistency of the results: carbon and redox balances were 96% ± 5% and 92% ± 7% (mean ± standard deviation for $n = 54$), respectively.

Growth parameters of steady-state chemostat cultures of ORS571 and U58 as a function of the DOT. The growth parameters of all types of chemostat cultures showed a similar dependency on the DOT in the range 0.2 to 3.0%. The growth yield on succinate, Y_{suc} (grams of DW mole of succinate^{-1}), for culture types 1 to 4 was plotted versus the DOT (Fig. 1A). All of the experimental data shown in Fig. 1A can be regarded as belonging to the same curve, along which the data from each of the four growth conditions are scattered. Thus, all 48 datum points were used to calculate a best fit, together with 95% confidence limits (Fig. 1A). The specific rate of succinate consumption (q_{suc} in millimoles of succinate gram of DW^{-1} h^{-1}) increased linearly with the DOT (Table 2). Because Y_{suc} is inversely proportional to q_{suc} ($Y_{suc} = \mu/q_{suc}$), Y_{suc} decreased hyperbolically with the DOT.

Similarly, the specific rates of O_2 consumption (qO_2 in millimoles of O_2 gram of DW^{-1} h^{-1}) and CO_2 production (qCO_2 in millimoles of CO_2 gram of DW^{-1} h^{-1}) for culture types 1 to 4 were plotted versus the DOT. When all of the experimental data were considered, both qO_2 and qCO_2 increased linearly with the DOT (Fig. 1B and C, respectively, with 95% confidence limits). Highly significant positive regressions between qO_2 or qCO_2 and the DOT were obtained (Table 2). The following conclusions can be drawn for chemostat culture types 1 to 4 (Fig. 1 and Table 2). (i) The growth parameters did change substantially: Y_{suc} decreased from 26.7 to 21.7 g of DW mol suc^{-1}, qO_2 increased from 7.4 to 10.6 mmol g of DW^{-1} h^{-1}, and qCO_2 increased from 10.4 to 14.3 mmol g of DW^{-1} h^{-1} in the range 0.2 to 3.0% O_2. Therefore, the efficiency of growth declined at increasing DOTs, i.e., at higher DOTs, more succinate was dissimilated (higher qO_2 and qCO_2) and less succinate was assimilated (lower Y_{suc}). (ii) ORS571 and U58 behaved similarly in the absence of H_2 in the influent gas flow. Hydrogen produced in cultures of the mutant gave rise to low partial H_2 pressures (±0.05% or ±0.20%, dependent on the gas flow rate), which apparently did not lead to inhibition of N_2 fixation. (iii) U58 cultures were not significantly affected by the presence of 2.5% H_2 in the influent gas flow. (iv) A fourfold decrease in the influent gas flow rate had no measurable effect on Y_{suc}, qO_2, and qCO_2 (see below). (v) The respiratory quotient was constant at 1.4 mol of CO_2/mol of O_2 over the range of 0.2 to 3.0% O_2.

H_2/N_2 ratio of steady-state chemostat cultures of U58 as a function of the DOT. In all chemostat cultures of ORS571 growing on N_2, H_2 was never observed in the effluent gas, owing to the presence of an active uptake hydrogenase. Hydrogenase-negative mutant strain U58, however, was not able to oxidize H_2, and H_2 accumulation in the effluent gas was monitored. Like qO_2, qCO_2, and q_{suc}, qH_2 was linearly dependent on the DOT (data not shown). For U58 cultures, the H_2/N_2 ratios were measured in culture types 1, 2, and 3 and these were plotted versus the DOT (Fig. 2). The H_2/N_2 ratio increased linearly from about 1.9 to 2.6 with increasing DOTs for culture types 1 and 3 and from 2.4 to 3.5 for type 2 cultures. These regressions were significant (Table 2), whereas the slopes themselves were not significantly different (F test; $P > 0.1$). From comparison of type 3 with type 1 cultures, differing only in the presence of 2.5% H_2 in the influent gas, a dissolved H_2 tension of around 2.7% had no significant effect on the H_2/N_2 ratio. In addition, from comparison of the 95% confidence limits, the H_2/N_2 ratios of type 2 cultures were significantly higher (about 30%) than those of culture types 1 and 3 over a DOT range of 0.4 to 3.0%. The only relevant difference between type 2 and type 1 and 3 cultures was the flow rate of the influent gas.

Estimation of ATP/N_2 and $ATP/2e^-$ ratios as a function of the DOT. The ATP/N_2 ratio is defined as the moles of ATP needed for reduction of 1 mol of N_2 with NAD(P)H as the

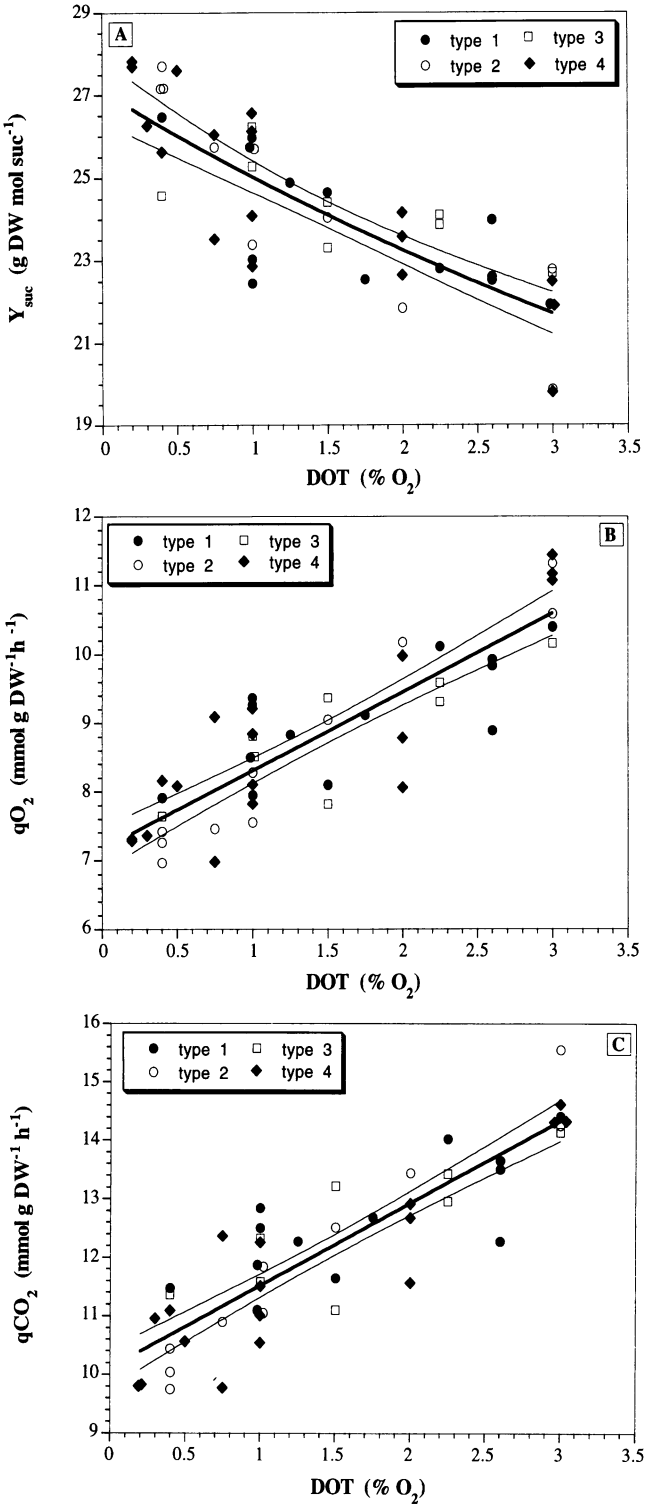

FIG. 1. Y_{suc} (A), qO_2 (B), and qCO_2 (C) versus DOT for 48 steady-state chemostat cultures of *A. caulinodans* ORS571 and U58. Table 1 describes the growth conditions of each particular culture (types 1 to 4). A hyperbolic fit is shown for Y_{suc}, and linear fits are shown for qO_2 and qCO_2 (thick lines), together with their 95% confidence limits (thin lines).

substrate (32). This ratio can be calculated from the comparison of Y_{ATP} (grams of DW per mole of ATP), MW_{C_1} (molecular weight of the biomass on a C_1 basis), and N_{C_1} (N content of the biomass on a C_1 basis) for growth on NH_3 and N_2. In the formula $ATP/N_2 = [(2 \times MW_{C_1})/(N_{C_1} \times Y_{ATP})]^{N_2} - [(2 \times MW_{C_1})/(N_{C_1} \times Y_{ATP})]^{NH_3}$, the value of the second bracketed term was determined previously (11) to be 50 or 70 (moles of ATP consumed per mole of N_2 equivalent), assuming energy conservation in the NADH-ubiquinone oxidoreductase (site 1) and ubiquinol oxidase (site 2) segments alone or together with the cytochrome *c* oxidase (site 3) segment, respectively. The parameters MW_{C_1} and N_{C_1} of the first bracketed term were calculated from the relevant data in the first paragraph of Results. Y_{ATP} was calculated from the fitted curve of Y_{suc} versus the DOT (Fig. 1A) by using the growth model previously developed (11). Y_{ATP}, and thus also ATP/N_2, is dependent on the efficiency of oxidative phosphorylation. NADH-ubiquinone oxidoreductase and ubiquinol oxidases are probably all involved in energy transduction during growth on N_2 in the range of 0.2 to 3.0% DOT (33). For growth on N_2, it is unknown whether or not cytochrome *c* oxidases are active in energy conservation. Hence, the ATP/N_2 ratio was calculated versus the DOT from Y_{ATP} values assuming energy conservation in the NADH-ubiquinone oxidoreductase and ubiquinol oxidase segments alone (Fig. 3A, broken lines), or together with the cytochrome *c* oxidase segment (Fig. 3B, solid lines), at each DOT. Alternatively, energy conservation at the cytochrome *c* oxidase segment might appear or disappear with increasing DOTs. A linear increase (Fig. 3A, solid lines) and a linear decrease (Fig. 3B, broken lines) of energy transduction at the cytochrome *c* oxidase segment with the DOT were taken as two typical examples among all possible mechanisms for activating or deactivating energy conservation in this segment. For each of the four options concerning growth on N_2, calculations were done by using the following four possible energy transduction scenarios with respect to growth on NH_3: I, sites 1 and 2 active at each DOT; II, sites 1, 2, and 3 active at each DOT; III, linear increase from sites 1 and 2 to sites 1, 2, and 3; IV, linear decrease from sites 1, 2, and 3 to sites 1 and 2. Thus, Fig. 3 shows four N_2 "butterflies," the contours of each of which are formed by four NH_3 lines.

It can be seen that the ATP/N_2 ratio increases in all of the cases shown in Fig. 3A and B, except for curves a′, c′, and d′ of Fig. 3B. Lines a′ and d′ of Fig. 3B show a more or less constant ATP/N_2 ratio, and line c′ shows a gradually decreasing ATP/N_2 ratio. Thus, in only 3 of 16 cases did the ATP/N_2 ratio not increase. These exceptions represent situations in which energy transduction gradually declines from three to two sites for growth on N_2 and is constant with two (a′) or 3 (d′) sites or increases from two to three (c′) sites for growth on NH_3.

From the ATP/N_2 ratio, the $ATP/2e^-$ ratio can be calculated by using the formula $ATP/2e^- = (ATP/N_2)/[(3 + (H_2/N_2)]$. The meaning of $ATP/2e^-$ was previously defined. The H_2/N_2 ratio was calculated from the fitted curve of the H_2/N_2 ratio versus the DOT (Fig. 2; at 5 liters/h). The dependencies of the $ATP/2e^-$ ratio on the DOT (data not shown) are very similar to those seen in Fig. 3. The $ATP/2e^-$ ratios increase in all cases, with the three exceptions mentioned above. In the latter cases, the $ATP/2e^-$ ratios slightly decrease. Interpretation of these results relies heavily on adoption of the concept of either respiratory protection (18, 41) or autoprotection (35), as will be argued in the Discussion.

TABLE 2. Summary of linear regressions and statistical parameters

Growth parameter	Linear regression ($y = a + bx$)	SE of regression slope (b)	F value[a]	P value (ϕ_1, ϕ_2 degrees of freedom)
q_{suc} (culture types 1–4)	3.69 + 0.31DOT	0.027	126	<0.005 (1, 11)
qO_2 (culture types 1–4)	7.16 + 1.15DOT	0.082	194	<0.005 (1, 11)
qCO_2 (culture types 1–4)	10.11 + 1.41DOT	0.088	253	<0.005 (1, 11)
H_2/N_2 ratio(5 liters/h)[b]	1.78 + 0.29DOT	0.040	54	<0.005 (1, 6)
H_2/N_2 ratio (20 liters/h)[b]	2.19 + 0.44DOT	0.113	15	<0.025 (1, 4)

[a] Determined by the F test for significance of regression slopes.
[b] Influent gas flow rate.

DISCUSSION

Previous investigations have described hydrogenase-negative mutants of *A. caulinodans* (5) constructed from a spontaneous mutant, ORS571-CY1, which is not capable of effective symbiotic N_2 fixation (17) and which accumulates large amounts (25 to 30%, wt/wt) of PHB (11). In the present investigation, U58, an isogenic hydrogenase-negative mutant of the wild type of *A. caulinodans*, ORS571, was used.

Growth on N_2 took place with declining efficiency at increasing DOTs. This loss of efficiency was accompanied by the observed statistically significant increase in the H_2/N_2 ratio. The cause of the rise in the H_2/N_2 ratio cannot be easily explained, as the following reasoning will demonstrate. A kinetic model for N_2 reduction has been constructed on the basis of in vitro experiments with purified nitrogenase reductase and nitrogenase from *Klebsiella pneumoniae*, in which dithionite was used as the electron donor and MgATP was used as the energy source (22, 23, 36–38). While experimental conditions that yield a slow electron flux through nitrogenase favor the reduction of H^+ above N_2 in vitro (4, 16, 22, 36, 38), whether extrapolation of in vitro results to the in vivo situation is valid for all properties of nitrogenase has been questioned (14, 15, 20). From our steady-state data, the sum of the specific rates of N_2 and H^+ consumption, expressed in electron equivalents per gram of DW per hour, increased at increasing DOTs. However, the H_2/N_2 ratio also increased. The sum of the nitrogenase reductase and nitrogenase contents of the bacterial dry mass did not increase with the DOT (11). If this pertained to nitrogenase content alone, in our in vivo system, H_2 production would then increase with increasing flux through nitrogenase, in contrast to the in vitro observations.

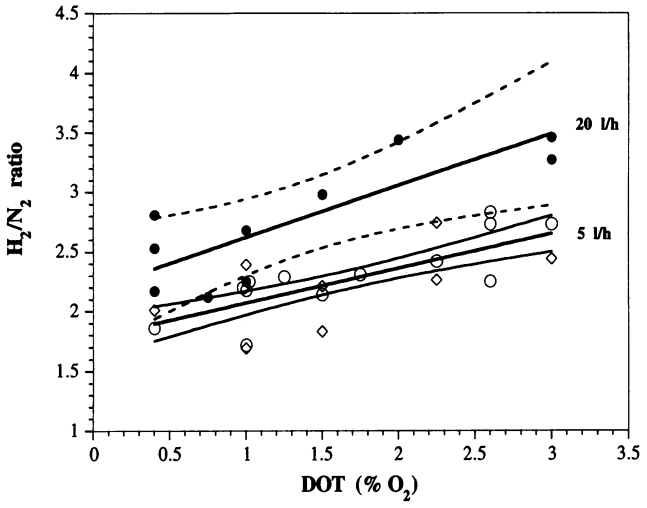

FIG. 2. H_2/N_2 ratio versus DOT for steady-state chemostat cultures of *A. caulinodans* U58. Table 1 describes the growth conditions of culture types 1, 2, and 3. Linear fits are shown for type 2 (●) cultures (n = 10) and for type 1 (○) and 3 (◇) (n = 21) cultures, together with their 95% confidence belts (closed symbols, – –; open symbols, ——).

With regard to the extent of H_2 production, it is worthwhile noting that the flow rate of the gas apparently affected the H_2/N_2 ratio: at 5 liters/h, the H_2/N_2 ratio was significantly lower than at 20 liters/h. The only relevant difference between these cultures seems to be in the concentrations of dissolved CO_2 and HCO_3^-, which were about four times higher at a low gas flow rate. It might be suggested that higher intracellular concentrations of these substances lead to lower nitrogenase-catalyzed H_2 production.

Our study revealed no significant effect of the presence of H_2 on the efficiency of growth of the hydrogenase-negative mutant. Neither H_2 produced through nitrogenase nor externally added H_2 (2.5%) had an effect on growth of the mutant. Nevertheless, it has long been recognized that H_2 may inhibit the process of N_2 fixation. For example, H_2 is known to be a competitive inhibitor of N_2 reduction in vitro, increasing the apparent K_m for N_2 in *K. pneumoniae* (23). In all probability, the partial H_2 pressures that were developed in our chemostat cultures (0.2 and 2.7%, respectively) were too low to affect N_2 fixation.

Although the rise in the H_2/N_2 ratio was significant, it was too small to account for all of the loss of growth efficiency. As mentioned before, the dependencies of the ATP/N_2 ratio and the ATP/$2e^-$ ratio on the DOT can be interpreted in terms of either respiratory protection or autoprotection. Respiratory activity as a protective device to prevent O_2 inhibition of nitrogenase activity is most highly developed in *Azotobacter* sp. (18). This diazotroph exhibits 10-fold higher rates of respiration than *A. caulinodans* (27). A crucial component of the concept of respiratory protection is that an increase of qO_2 is coupled with changes in the levels and activities of components of a branched respiratory chain in such a way that the efficiency of energy transduction is lowered. Because *A. caulinodans* has at least four different oxidases, two quinol oxidases and two cytochrome *c* oxidases (19), at its disposal, it might adjust the efficiency of energy transduction in accordance with its needs.

Changes in the reduction levels of the cytochrome *b* and *c* pools with increasing DOTs indeed suggest that alterations in electron transfer routes to O_2 might occur (29). However, the specific changes in the respiratory chain which take place with increasing DOTs are unknown. Nevertheless, the assumption that a gradual loss of energy transduction with increasing DOTs occurs in the cytochrome *c* oxidase segment of the respiratory chain would explain the lower efficiency growth on N_2, for example. In that case, the ATP/N_2 ratio would remain more or less constant (Fig. 3B; curves a′ and d′) or even

slightly decrease (curve c'). As a result, the overall ATP/2e$^-$ ratio would have to decrease slightly with increasing DOTs, because the H_2/N_2 ratio increased.

To sum up, the overall efficiency of N_2 fixation would remain constant and the increase in the respiration rate would just be balanced out by the decline in the efficiency of oxidative phosphorylation; the gradual loss of growth efficiency with increasing DOTs is caused mainly by a gradual decrease in the P/O ratio.

Alternatively, autoprotection might be responsible for part of the decrease in growth efficiency. Autoprotection is defined as the ability of nitrogenase reductase to reduce O_2 without being inactivated, when O_2 is not in excess (35). If reduction of O_2 by nitrogenase reductase occurred at a rate proportional to the DOT, the cell would repeatedly reduce the nitrogenase reductase at the expense of energy. As a result, the overall ATP/2e$^-$ ratio and ATP/N_2 ratio would appear to increase. This explanation makes sense where efficiency of energy transduction is constant or increases with rising DOTs, because in that case the ATP/N_2 ratio indeed increases, irrespective of the energy transduction scenario chosen for growth on NH_3 (Fig. 3A, curves a to d and a' to d'; Fig. 3B, curves a to d). In one case, this holds true even if energy conservation decreases with rising DOTs (Fig. 3B, curve b'). Likewise, the ATP/2e$^-$ ratio versus the DOT, as calculated from the H_2/N_2 ratio and the ATP/N_2 ratio, would increase (data not shown).

In summary, the overall efficiency of N_2 fixation would decline and a substantial proportion of the increase in the respiration rate would be needed to provide the energy for the repeated reduction of nitrogenase reductase (which has transferred its electron to O_2). The gradual loss of growth efficiency is caused mainly by a gradual decrease in the overall efficiency of N_2 fixation.

Although the data presented in this report do not per se lead to a preference for either explanation, there is circumstantial evidence in favor of autoprotection. (i) The fact that a 10-fold increase in the DOT merely resulted in a 1.4-fold increase in qO_2 might indicate that the intracellular DOT was similar to the regulated DOT in the bulk phase. Thus, the intracellular O_2 concentration (dependent on the intracellular DOT and the solubility of O_2 in the bacterial cytoplasm) might be substantial. In addition, high concentrations of nitrogenase reductase (60 to 375 μM) have been observed in aerobic N_2-fixing bacteria and bacteroids (9, 15, 20, 35). Thus, a direct interaction between nitrogenase reductase and O_2 is conceivable.

(ii) N_2-fixing steady-state cultures were readily achieved at a dilution rate of 0.1 h^{-1} up to a DOT of 3.0% but not higher. In our experience, the steady states occasionally formed in the range from 3.0 to 4.0% dissolved O_2 were easily disturbed. Excess O_2 (a more-than-fourfold excess of O_2 over nitrogenase reductase) inactivates the nitrogenase reductase rather quickly in vitro by production of the superoxide anion radical (35). If this reaction also occurred in vivo and if intracellular O_2 were in excess of nitrogenase reductase starting from 3 to 4% DOT, accumulation of this toxic O_2 metabolite might inactivate the nitrogenase reductase and thereby cause the culture to wash out.

(iii) Regulation of cytochrome aa_3 oxidase activity by O_2 has been noticed for some rhizobia growing on combined nitrogen. The cytochrome aa_3 oxidase activity of *A. caulinodans*, measured as β-glucuronidase activity, was strongly expressed during exponential growth in batch culture in O_2-rich environments and then deactivated before onset of the stationary phase, in which the DOT was presumably lowered (19). In *A. caulinodans* chemostat cultures, cytochrome aa_3 also increased as the DOT increased (11, 33). Similarly, cytochrome aa_3 was found to be regulated by O_2 in *Bradyrhizobium japonicum*, the activity being highest under fully aerobic conditions (12). Hence, cytochrome aa_3 expression in free-living bacteria seems to be induced at increased DOTs. Activation of energy transduction in the cytochrome *c* oxidase segment in the range of 0.2 to 3.0% DOT during growth on N_2, as well as NH_3, would support the concept of autoprotection (Fig. 3A, curve c).

Furthermore, recently induction of an alternative cytochrome *c* oxidase, a member of the heme/copper cytochrome oxidase superfamily, has been shown to occur in *B. japonicum* under microaerobic conditions (28). Most likely, *A. caulinodans* also expresses this alternative oxidase because it contains a similar fixNOPQ region (24). It is unknown whether this oxidase is a proton pump or not.

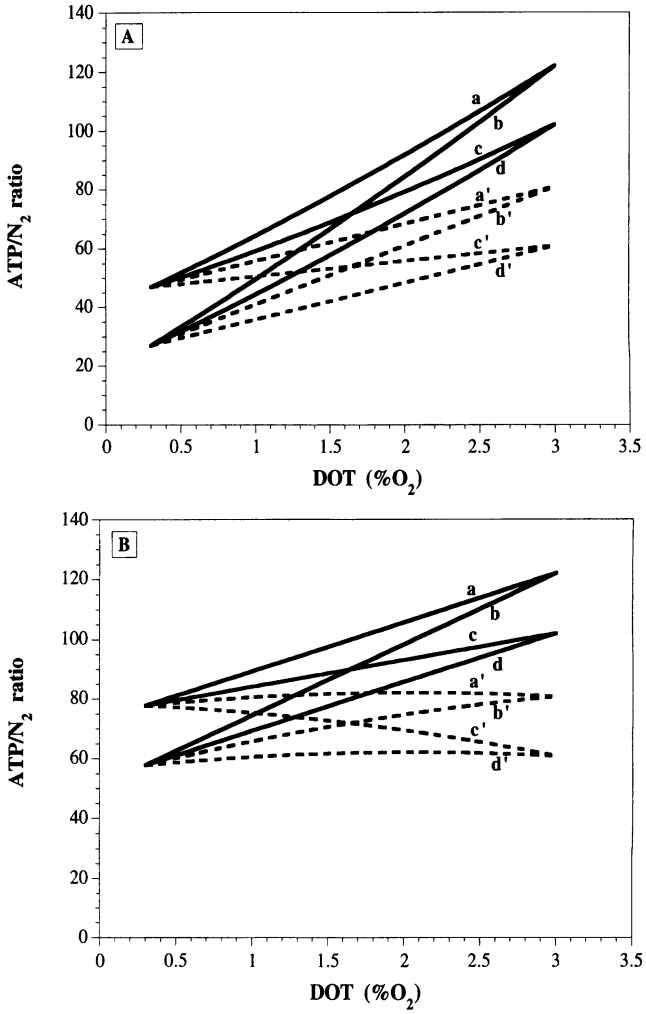

FIG. 3. Calculated ATP/N_2 ratios versus DOT. ATP/N_2 ratios were determined under four different assumptions on changes in P/O ratios at increasing DOTs for growth on N_2 (four N_2 butterflies). (A) Lines: a to d, linear increase from two to three sites; a' to d', two sites at each DOT. (B) Lines: a to d, three sites at each DOT; a' to d', linear decrease from three to two sites. The contour of each butterfly was formed by using the following four different energy transduction scenarios for growth on NH_3: a and a', two sites at each DOT; b and b', linear decrease from three to two sites; c and c', linear increase from two to three sites; d and d', three sites at each DOT.

However, it must be stressed that regulation of cytochrome aa_3 and/or alternative cytochrome *c* oxidase activity might be different in cultures that fix N_2. In chemostat cultures of *A. caulinodans* growing on N_2, the A_{605} peak observed in difference spectra, which is a measure of the amount of cytochrome aa_3, is barely visible under O_2-limited conditions (33) and comparatively small in the range of 0.3 to 3.0% DOT (11). Still, in cells grown on N_2 at a low DOT, flash photolysis of CO-reduced spectra resulted in the reappearance of a small peak at 445 nm indicative of cytochrome aa_3 (33).

All in all, the decline in growth efficiency with increasing DOTs can be explained only for a minor part by the increase in the H_2/N_2 ratio and both respiratory protection and autoprotection can be put forward to explain the remaining major part. Although circumstantial evidence in favor of autoprotection exists, from the data presented in this report, no definite choice can be made between these physiological concepts and further research is needed to test both hypotheses.

ACKNOWLEDGMENTS

We are grateful to U. Hilgert and F. J. de Bruijn for construction of the isogenic hydrogenase-negative mutant of *A. caulinodans* ORS571. We thank E. W. de Vrind-de Jong and J. P. M. de Vrind for constructive criticism of the manuscript and N. J. Taylor for improvement of English usage.

This investigation was supported by the Netherlands Foundation for Biological Research (BION) with financial aid from the Netherlands Organization for Scientific Research (NWO).

REFERENCES

1. **Allen, G. C., D. T. Grimm, and G. H. Elkan.** 1991. Oxygen uptake and hydrogen-stimulated nitrogenase activity from *Azorhizobium caulinodans* ORS571 grown in a succinate-limited chemostat. Appl. Env. Microbiol. **57:**3220–3225.
2. **Andersen, K., and K. T. Shanmugam.** 1977. Energetics of biological nitrogen fixation: determination of the ratio of formation of H_2 to NH_4^+ catalysed by nitrogenase of *Klebsiella pneumoniae in vivo*. J. Gen. Microbiol. **103:**107–122.
3. **Bergersen, F. J., G. L. Turner, D. Bogusz, Y. Q. Wu, and C. A. Appleby.** 1986. Effects of O_2 concentration and various haemoglobins on respiration and nitrogenase activity of bacteroids from stem and root nodules of *Sesbania rostrata* and of the same bacteria from continuous cultures. J. Gen. Microbiol. **132:**3325–3336.
4. **Davis, L. C., V. K. Shah, and W. J. Brill.** 1975. Nitrogenase. Effects of component ratio, ATP and H_2 on the distribution of electrons to alternative substrates. Biochim. Biophys. Acta **403:**67–78.
5. **De Vries, W., J. Ras, H. Stam, M. M. A. van Vlerken, U. Hilgert, F. J. de Bruijn, and A. H. Stouthamer.** 1988. Isolation and characterization of hydrogenase-negative mutants of *Azorhizobium caulinodans* ORS571. Arch. Microbiol. **150:**595–599.
6. **De Vries, W., H. Stam, A. J. M. Ligtenberg, L. H. Simons, and A. H. Stouthamer.** 1986. The effect of the dissolved oxygen concentration and anabolic limitations on the behaviour of *Rhizobium* ORS571 in chemostat cultures. Antonie van Leeuwenhoek **52:**85–96.
7. **De Vries, W., H. Stam, and A. H. Stouthamer.** 1984. Hydrogen oxidation and nitrogen fixation in rhizobia, with special attention focused on strain ORS571. Antonie van Leeuwenhoek **50:**505–524.
8. **de Vries, W., and A. H. Stouthamer.** 1968. Fermentation of glucose, lactose, galactose, mannitol, and xylose by bifidobacteria. J. Bacteriol. **96:**472–478.
9. **Dingler, C., J. Kuhla, H. Wassink, and J. Oelze.** 1988. Levels and activities of nitrogenase proteins in *Azotobacter vinelandii* at different dissolved oxygen concentrations. J. Bacteriol. **170:**2148–2152.
10. **Dreyfus, B., J. L. Garcia, and M. Gillis.** 1988. Characterization of *Azorhizobium caulinodans* gen. nov., sp. nov., a stem-nodulating nitrogen-fixing bacterium isolated from *Sesbania rostrata*. Int. J. Syst. Bacteriol. **38:**89–98.
11. **Ferdinandy-van Vlerken, M. M. A.** 1990. Ph.D. thesis. Vrije Universiteit, Amsterdam, The Netherlands.
12. **Gabel, C., and R. J. Maier.** 1993. Oxygen-dependent transcriptional regulation of cytochrome aa_3 in *Bradyrhizobium japonicum*. J. Bacteriol. **175:**128–132.
13. **Gebhardt, C., G. L. Turner, A. H. Gibson, B. L. Dreyfus, and F. J. Bergersen.** 1984. Nitrogen-fixing growth in continuous culture of a strain of *Rhizobium* sp. isolated from stem nodules on *Sesbania rostrata*. J. Gen. Microbiol. **130:**843–848.
14. **Haaker, H., and J. Klugkist.** 1987. The bioenergetics of electron transport to nitrogenase. FEMS Microbiol. Rev. **46:**57–72.
15. **Haaker, H., and H. Wassink.** 1984. Electron allocation to H^+ and N_2 by nitrogenase in *Rhizobium leguminosarum* bacteroids. Eur. J. Biochem. **142:**37–42.
16. **Hageman, R. V., and R. H. Burris.** 1980. Electron allocation to alternative substrates of *Azotobacter* nitrogenase is controlled by the electron flux through dinitrogenase. Biochim. Biophys. Acta **591:**63–75.
17. **Hilgert, U.** 1991. Ph.D. thesis. Ruhr-Universität, Bochum, Germany.
18. **Hill, S.** 1988. How is nitrogenase regulated by oxygen? FEMS Microbiol. Rev. **54:**111–130.
19. **Kitts, C. L., and R. A. Ludwig.** 1994. *Azorhizobium caulinodans* respires with at least four terminal oxidases. J. Bacteriol. **176:**886–895.
20. **Klugkist, J., H. Haaker, H. Wassink, and C. Veeger.** 1985. The catalytic activity of nitrogenase in intact *Azotobacter vinelandii* cells. Eur. J. Biochem. **146:**509–515.
21. **Law, J. H., and R. A. Slepecky.** 1961. Assay of poly-β-hydroxybutyric acid. J. Bacteriol. **82:**33–36.
22. **Lowe, D. J., and R. N. F. Thorneley.** 1984. The mechanism of *Klebsiella pneumoniae* nitrogenase action. Pre-steady-state kinetics of H_2 formation. Biochem. J. **224:**877–886.
23. **Lowe, D. J., and R. N. F. Thorneley.** 1984. The mechanism of *Klebsiella pneumoniae* nitrogenase action. The determination of rate constants required for the simulation of the kinetics of N_2 reduction and H_2 evolution. Biochem. J. **224:**895–901.
24. **Mandon, K., P. A. Kaminski, C. Mougel, N. Desnoues, B. Dreyfus, and C. Elmerich.** 1993. Role of the fixGHI region of *Azorhizobium caulinodans* in free-living and symbiotic nitrogen fixation. FEMS Microbiol. Lett. **114:**185–190.
25. **Noorman, H. J., G. C. A. Luijkx, K. C. A. M. Luyben, and J. J. Heijnen.** 1992. Modeling and experimental validation of carbon dioxide evolution in alkalophilic cultures. Biotechnol. Bioeng. **39:**1069–1079.
26. **O'Brian, M. R., and R. J. Maier.** 1988. Hydrogen metabolism in *Rhizobium*: energetics, regulation, enzymology and genetics. Adv. Microb. Physiol. **29:**1–52.
27. **Post, E., D. Kleiner, and J. Oelze.** 1983. Whole cell respiration and nitrogenase activities in *Azotobacter vinelandii* growing in oxygen controlled continuous culture. Arch. Microbiol. **134:**68–72.
28. **Preisig, O., D. Anthamatten, and H. Hennecke.** 1993. Genes for a microaerobically induced oxidase complex in *Bradyrhizobium japonicum* are essential for a nitrogen-fixing endosymbiosis. Proc. Natl. Acad. Sci. USA **90:**3309–3313.
29. **Pronk, A. F., F. C. Boogerd, C. Stoof, L. F. Oltmann, A. H. Stouthamer, and H. W. van Verseveld.** 1993. *In situ* determination of the reduction levels of cytochromes *b* and *c* in growing bacteria: a case study with N_2-fixing *Azorhizobium caulinodans*. Anal. Biochem. **214:**149–155.
30. **Riis, V., and W. Mai.** 1988. Gas chromatographic determination of poly-β-hydroxybutyric acid in microbial biomass after hydrochloric acid propanolysis. J. Chromatogr. **445:**285–289.
31. **Simpson, F. B., and R. H. Burris.** 1984. A nitrogen pressure of 50 atmospheres does not prevent evolution of hydrogen by nitrogenase. Science **224:**1095–1097.
32. **Stam, H., A. H. Stouthamer, and H. W. van Verseveld.** 1987. Hydrogen metabolism and energy costs of nitrogen fixation. FEMS Microbiol. Rev. **46:**73–92.
33. **Stam, H., H. W. van Verseveld, W. de Vries, and A. H. Stouthamer.** 1984. Hydrogen oxidation and efficiency of nitrogen fixation in succinate-limited chemostat cultures of *Rhizobium* ORS571. Arch. Microbiol. **139:**53–60.
34. **Stouthamer, A. H., H. Stam, W. de Vries, and M. van Vlerken.** 1988. Some aspects of nitrogen fixation in free-living cultures of

Rhizobium, p. 257–261. *In* H. Bothe, F. J. de Bruijn, and W. E. Newton (ed.), Nitrogen fixation: hundred years after. Proceedings of the 7th International Congress on Nitrogen Fixation, Köln, F.R.G. Gustav Fischer, Stuttgart, Germany.

35. **Thorneley, R. N. F., and G. A. Ashby.** 1989. Oxidation of nitrogenase iron protein by dioxygen without inactivation could contribute to high respiration rates of *Azotobacter* species and facilitate nitrogen fixation in other aerobic environments. Biochem. J. **261:**181–187.
36. **Thorneley, R. N. F., and D. J. Lowe.** 1983. Nitrogenase of *Klebsiella pneumoniae*. Kinetics of the dissociation of oxidized iron protein from molybdenum-iron protein: identification of the rate-limiting step for substrate reduction. Biochem. J. **215:**393–403.
37. **Thorneley, R. N. F., and D. J. Lowe.** 1984. The mechanism of *Klebsiella pneumoniae* nitrogenase action. Pre-steady-state kinetics of an enzyme-bound intermediate in N_2 reduction and of NH_3 formation. Biochem. J. **224:**887–894.
38. **Thorneley, R. N. F., and D. J. Lowe.** 1984. The mechanism of *Klebsiella pneumoniae* nitrogenase action. Simulation of the dependence of H_2-evolution rate on component-protein concentration and ratio and sodium dithionite concentration. Biochem. J. **224:**903–909.
39. **Van der Aar, P. C., A. H. Stouthamer, and H. W. van Verseveld.** 1989. Possible misconceptions about O_2 consumption and CO_2 production measurements in stirred microbial cultures. J. Microbiol. Methods **9:**281–286.
40. **Van Verseveld, H. W., J. A. de Hollander, J. Frankena, M. Braster, F. J. Leeuwerik, and A. H. Stouthamer.** 1986. Modelling of microbial substrate conversion, growth and product formation in a recycling fermentor. Antonie van Leeuwenhoek **52:**325–342.
41. **Yates, M. G.** 1988. The role of oxygen and hydrogen in nitrogen fixation, p. 383–416. *In* J. A. Cole and S. J. Ferguson (ed.), The nitrogen and sulphur cycles: 52nd Symposium of the Society for General Microbiology. Cambridge University Press, Cambridge.